A Glucose-6-Phosphate/Phosphate Translocator Is Involved in Carbohydrate Metabolism and Starch Biosynthesis in Sweet Potato *(Ipomoea Batatas* (L.) Lam.)

Zhengdan Wu
Southwest University
Zhiqian Wang
Southwest University
Kai Zhang (zhangkai2010s@163.com)
Southwest University

Research Article

Keywords: sweet potato, glucose-6-phosphate/phosphate translocator, starch

Posted Date: September 29th, 2021

DOI: https://doi.org/10.21203/rs.3.rs-927302/v1

Abstract

Sweet potato (*Ipomoea batatas* (L.) Lam.) is a good source of carbohydrates, an excellent raw material for starch-based industries, and a strong candidate for biofuel production due to its high starch content. However, the molecular basis of starch biosynthesis and accumulation in sweet potato is still insufficiently understood. Glucose-6-phosphate/phosphate translocators (GPTs) mediate the import of glucose-6-phosphate (Glc6P) into plastids for starch synthesis. Here, we report the isolation of a GPT-encoding gene, *IbG6PPT1*, from sweet potato and the identification of two additional *IbG6PPT1* gene copies in the sweet potato genome. *IbG6PPT1* encodes a chloroplast membrane–localized GPT belonging to the GPT1 group and highly expressed in storage root of sweet potato. Heterologous expression of *IbG6PPT1* resulted in increased starch content in the leaves, root tips, and seeds and soluble sugar in seeds of *Arabidopsis thaliana*, but a reduction in soluble sugar in the leaves. These findings suggested that IbG6PPT1 might play a critical role in carbohydrate accumulation in storage tissues and would be a good candidate gene for controlling critical starch properties in sweet potato.

Background

Sweet potato (*Ipomoea batatas* (L.) Lam.) is an important food crop that is cultivated in over 100 countries due to its stable yield, rich nutrient content, low input requirements, multiple uses, high yield potential, and adaptability under a range of environmental conditions (Burri, 2011; Hu et al., 2003; Mitra, 2012; Yang et al., 2020; Zhang et al., 2017). Sweet potato is grown mainly for its edible, starchy storage root, which is 50–80% starch by dry matter (Zhou et al., 2015). This high starch content renders sweet potato a good source of carbohydrates, an excellent raw material for starch-based industries, and a strong candidate as an inexpensive raw material for biofuel production (Koçar and Civaş, 2013; Nedunchezhiyan et al., 2012; Srichuwong et al., 2012). Although sweet potato is one of the top starch-rich root crops worldwide (Wang et al., 2019), the molecular basis of starch biosynthesis and accumulation in this species is poorly understood.

Starch is synthesized in plants through a complex pathway involving multiple enzymes and transporters (Lai et al., 2016; Schreiber et al., 2014; Zhang et al., 2017). Starch biosynthesis begins with the synthesis of sucrose, the major product of photosynthesis, in source tissues. During this process, sucrose can be converted to glucose-6-phosphate (Glc6P) and then imported into the plastid by glucose-6-phosphate/phosphate translocators (GPTs), proteins belonging to the transporter subfamily of phosphate translocators (PTs).

Two functional GPT genes have been identified in Arabidopsis (*Arabidopsis thaliana*). GPT1 is localized on the inner envelope of the plastid membrane and transports Glc6P into plastids for use in starch biosynthesis, the oxidative pentose phosphate pathway (OPPP), and fatty acid biosynthesis (Kunz et al., 2010). GPT1 is also localized to peroxisomes, where it preferentially exchanges Glc6P for ribulose-5-phosphate (Ru5P) (Baune et al., 2020).

GPTs play important roles in several physiological processes. Arabidopsis *GPT1* is essential for the development of male and female gametophytes, embryos, and seeds (Chen et al., 2019; Zhang et al., 2020). GPT1 is highly expressed at the late stages of pollen development, where it drives Glc6P from the cytosol and into plastids for fatty acid biosynthesis, and thus plays an important role in lipid body biogenesis during pollen maturation (Zheng et al., 2018). By contrast, Arabidopsis *GPT2* is expressed when photosynthesis is increased by light, which allows increased net import of Glc6P from the cytosol to chloroplasts, thus facilitating starch synthesis during stochastic high-light conditions (Dyson et al., 2015; Weise et al., 2019). *GPT2* responds rapidly by glucose and sucrose induced and plays an essential role in interpreting environmental signals (Chen et al., 2019; Weise et al., 2019). GPT1 plays a major role in the regulation of starch synthesis in other plants. GPT1 in Narbonne vetch (*Vicia narbonensis*) is critical for starch synthesis and storage in developing seeds. In *Vicia* transgenic plants expressing antisense GPT1 via *Agrobacterium*-mediated transformation, amyloplasts developed later and were smaller in size, starch biosynthesis was reduced, and storage protein biosynthesis increased (Rolletschek et al., 2007). In rice, pollen grains from homozygous *osgpt1* mutant plants fail to accumulate starch granules, resulting in pollen sterility (Qu et al., 2021). However, the role of GPTs in sweet potato has not been investigated.

In our previous work, we identified *GPT* genes in sweet potato using transcriptome analysis and showed that they have different expression patterns during storage root development and among sweet potato genotypes with different starch properties. Therefore, these GPTs are probably involved in starch accumulation and sucrose metabolism in sweet potato (Zhang et al., 2017). Here, we cloned two *GPT* genes and analyzed their protein localizations, sequence features, and functions. Our results provide important insights into the mechanisms underlying the starch properties of sweet potato.

Results

Two GPT-encoding genes were cloned from sweet potato

To ensure that the full-length mRNA sequence of sweet potato *GPT* genes could be obtained, the RACE method was used for cloning. Two cDNA sequences encoding the sweet potato *GPT* genes were obtained, named *IbG6PPT1* and *IbG6PPT1-2*. The obtained sequences contained 1763 and 1767 bp of mRNA, corresponding to 1191 and 1200 bp of ORFs and encoding 399-aa and 396-aa protein sequences, respectively. The two genes shared 96.627%, 98.083%, and 98.747% identity at the mRNA, CDS, and putative amino acid levels, respectively. The two proteins differed in only five amino acids (Fig. 1), including a deletion of the $L_{37}P_{38}A_{39}$ sequence in the shorter GPT.

The sweet potato genome is annotated with three *GPT1* gene members: *IbG6PPT1* located on chromosome 3 (chr3), *IbG6PPT1-2* located on chr2, and another *IbG6PPT1*-like gene also expected to be located on chr2. However, the sequence of this *IbG6PPT1*-like gene was not cloned from our cDNA library. Amino acid differences between IbG6PPT1 and IbG6PPT1-2 were not located at conserved domains or important transmembrane domains, indicating that these proteins are likely functional.

The cloned GPT genes belong to the GPT1 group

The GPT subfamily is relatively well characterized at the molecular level. The GPT subfamily includes three groups: GPT1, GPT2, and GPT3 (Chadee and Vanlerberghe, 2020). The sweet potato *GPT* genes showed 98.75% and 97.99% identity with *Ipomoea nil* and *Ipomoea triloba* GPT1, respectively. A GPT phylogenetic tree showed that the GPT1 group consisted of two sweet potato GPT proteins as well as *Ipomoea trilobal*, morning glory (*Ipomoea nil*), tobacco (*Nicotiana tabacum*), potato (*Solanum tuberosum*), tomato (*Solanum lycopersicum*), China rose (*Rosa chinensis*), *Arabidopsis thaliana*, rice (*Oryza sativa*), and maize (*Zea mays*) GPT1 proteins. The GPT2 group consisted of AtGPT2, whereas the GPT3 group mainly consisted of two *N. tabacum* GTP3 proteins, XP_016451801.1 and XP_016454155.1 (Chadee and Vanlerberghe, 2020) (Fig. 2). Therefore, the obtained sweet potato GPTs belong to the GPT1 group.

The protein sequence alignment and phylogenetic tree showed that IbG6PPT1 was more similar than IbG6PPT1-2 to GPT1 proteins from *Ipomoea nil* and *Ipomoea triloba* (Fig. 1 and Fig. 2), indicating that *IbG6PPT1* might match previous GPT1 findings better in the *Ipomoea* genus. Thus, we focused on *IbG6PPT1* for the remainder of this work.

IbG6PPT1 is likely a chloroplast-located GPT

We created a GFP-tagged version of IbG6PPT1 and transiently expressed it in *N. benthamiana*. The GFP signal surrounded the chloroplast marker fluorescence, indicating that IbG6PPT1 localizes to the chloroplast membrane (Fig. 3). No signal peptide was predicted from the protein sequence, meaning that the protein wasn't secreted protein. TMPred and TMHMM predicted the presence of seven transmembrane helixes (Fig. 1), consistent with a role for IbG6PPT1 in Glc6P transport through the chloroplast membrane. Modeling of the three-dimensional (3D) structure of IbG6PPT1 predicted that two IbG6PPT1 proteins form a homodimer (Fig. 4). In addition, IbG6PPT1 contains a conserved sugar phosphate transporter domain (Jack et al., 2001). These results strongly suggest that IbG6PPT1 is a chloroplast membrane–localized, GPT family protein in sweet potato.

IbG6PPT1 is highly expressed in sweet potato storage root

We next attempted to determine whether and how strongly *IbG6PPT1* is expressed in various sweet potato tissues by extracting RNA from the petiole, stem, leaf, and storage root and performing RT-qPCR to quantify gene expression. *IbG6PPT1* was expressed in all tissues but showed its highest expression in storage roots, followed by the petiole, stem, and leaves (Fig. 5). Interestingly, the higher expression of *IbG6PPT1* in roots than in leaves suggests that it may function in Glc6P transport in non-green tissues rather than in photosynthetic tissues.

Heterologous expression of IbG6PPT1 affects starch and sucrose content

To identify the function of IbG6PPT1, we transformed a *p35S*::*IbG6PPT1*-YFP construct into wild-type (Col-0) Arabidopsis. Analysis of IbG6PPT1-YFP expression by qPCR and western blotting showed that the

fusion protein was heterologously expressed across four independent transgenic lines, designated OV-14, OV-30, OV-76, and OV-57, that were selected from the T_2 progeny, as well as in the wild type (Fig. 6a and 6b). There were no differences in growth and development between the transgenic progeny and the wild-type control (Fig. 6c).

In contrast to their wild-type-like appearance, the soluble sugar content in the leaves of the transgenic *IbG6PPT1-YFP* lines was only 76.59–83.40% of control (Fig. 7a, Table S1). Meanwhile, the leaves of the 6 weeks transgenic T_2 plants had a measured starch content 1.65- to 2.75-fold higher than the control (Fig. 7b, Table S1), which was confirmed by iodine staining in 3 weeks seedlings (Fig. 7c). Surprisingly, the 1000 seed weights of the transgenic lines were 1.06- to 1.19-fold higher than in the control plants (Fig. 7d, Table S1). Further analyses showed that the soluble sugar content and starch content in the seeds of transgenic *IbG6PPT1-YFP* lines were 1.20- to 1.47-fold and 1.13- to 1.31-fold higher than in the control plants, respectively (Fig. 7e and 7f, Table S1). In the root tips, iodine staining showed that the starch content of transgenic *IbG6PPT1-YFP* lines was higher than that in control plants (Fig. 7g and 7h). Above all, heterologous expression of the *IbG6PPT1* gene increased both starch and sucrose content in Arabidopsis.

Discussion

IbG6PPT1 is present in several gene copies that may have different functions

The sweet potato genome is allohexaploid ($2n = 6x = 90$), containing two B1 and four B2 component genomes (B1B1B2B2B2B2) (Gao et al., 2020; Yang et al., 2017; Zhang et al., 2020). Therefore, there may be up to six copies of each gene. In this study, we cloned two *GPT1* genes that share a high level of identity in both the mRNA and protein sequences (Fig. 1). However, we found three potential *IbG6PPT1* genes in the genome database, the two we cloned and another one on chr2 that might be a homolog or paralog of one of the cloned genes. During the evolution of sweet potato's polyploid genome, the duplicated genes might have developed expressional, regulatory, or functional divergence (Fan et al., 2017; Wesemael et al., 2018). Because of the very high sequence similarity between the *IbG6PPT1* genes, it is difficult to examine the expression pattern or function of a single such gene. Future work should investigate whether the three *IbG6PPT1* genes show functional divergence in Glc6 transport and thus play different roles in starch accumulation and sucrose metabolism in sweet potato. Alternately, they may not have diverged as strongly, and one gene's function may have been compensated for by the function of another gene. Future genetic engineering of the sweet potato will require gene function studies to determine the contribution of each gene copy to relevant phenotypes and identify the major gene controlling sweet potato starch properties.

IbG6PPT1 has similar functions to other GPT1 proteins

GPT1 proteins transport Glc6P into plastids for starch and/or fatty acid biosynthesis, depending on the plant species (Zheng et al., 2018). A previous report demonstrated that starch biosynthesis is mediated

by *VnGPT1* in pea embryos (Rolletschek et al., 2007). Starch is the major carbon storage molecule of sweet potato, accounting for 50–80% of dry matter in the storage root, the organ that determines sweet potato's economic value as a crop (Zhang et al., 2017), whereas fatty acids are almost undetectable. In Arabidopsis, fatty acid biosynthesis in pollen is controlled by regulating *AtGPT1* expression through the MKK4/MKK5-MPK3/MPK6 cascade and the downstream transcription factors WRKY2 and WRKY34 (Zheng et al., 2018). In rice, pollen grains from homozygous *osgpt1* mutant plants fail to accumulate starch granules, resulting in pollen sterility (Qu et al., 2021). Like *AtGPT1*, which is expressed ubiquitously throughout Arabidopsis development (Niewiadomski et al., 2005), we found that *IbG6PPT1* is expressed in both aboveground and underground organs in sweet potato (Fig. 5), suggesting potential functions in both autotrophic and heterotrophic tissues. The localization of IbG6PPT1 to the chloroplast membrane (Fig. 3) implied that it may function in transporting Glc6P from the cytosol into plastids.

To better elucidate the function of the *IbG6PPT1* gene in starch accumulation, we cloned *IbG6PPT1*, heterologously expressed it in Arabidopsis, and then measured starch accumulation in the resulting transgenic plants. *IbG6PPT1* expression increased starch accumulation in Arabidopsis leaves, seeds, and root tips, suggesting that it promotes starch biosynthesis. Lipid bodies and protein are the major storage compounds in mature Arabidopsis seeds, each accounting for up to 40% of the dry weight (Andriotis et al., 2010), whereas starch are lower. The weight of 1000 seed we observed in *IbG6PPT1*-expressing plant is greater than control plant, indicating that *IbG6PPT1* may also promote storage matter accumulation in Arabidopsis seeds.

IbG6PPT1 promotes carbohydrate accumulation in Arabidopsis storage tissues

Sucrose is a major end product of photosynthesis and the primary sugar transported within plants (Winter and Huber, 2000). In heterotrophic tissues, sucrose imported from photosynthetic tissues is converted to Glc6P, and some Glc6P can be transported into the plastid through GPTs for starch and/or fatty acid biosynthesis. Another portion of the Glc6P is metabolized in the cytosol to phosphoenolpyruvate (PEP), which is essential for the biosynthesis of lipids and other storage substances (Lee et al., 2017). In *IbG6PPT1*-expressing Arabidopsis, the starch content in the leaves increased significantly, while the soluble sugar content was reduced, compared to that in control plants (Fig. 7). Thus, heterologous expression of *IbG6PPT1* promoted starch accumulation and sucrose metabolism, probably due to the high expression of GPT, which would be expected to increase the level of Glc6P imported into the chloroplast or amyloplast for starch synthesis. *IbG6PPT1* expression in Arabidopsis would promote Glc6P transport into plastids for storage and thus contribute to the observed carbohydrate accumulation in transgenic seeds compared with controls. Therefore, it is also likely that *IbG6PPT1* plays a critical role in metabolic distribution and carbohydrate accumulation in storage tissues. This also indirectly implies that *IbG6PPT1* plays an important role in the accumulation of substances in the storage roots of sweet potatoes.

IbG6PPT1 enhances transport activity from sink to source

In plants heterologously expressing *IbG6PPT1*, the starch contents in leaves, seeds, and root tips increased (Fig. 7), indicating that IbG6PPT1 might have high activity in Glc6P transport and play an important role in starch biosynthesis. Sweet potato is one of the top starch-rich root crops globally (Wang et al., 2019). To ensure starch storage in the storage root, any increases in photosynthetic activity depend on corresponding development of carbon sink capacity. Thus, Glc6P transporters such as IbG6PPT1 should exhibit a high capacity for photosynthate transport. Indeed, heterologous expression of *IbG6PPT1* increased the starch content in the leaves, seeds, and root tips in Arabidopsis. However, expression did not affect the growth and development of transgenic plants, suggesting the potential of IbG6PPT1 to promote starch accumulation in other crops.

Conclusion

The changes in starch and sugar content of transgenic Arabidopsis plants showed that IbG6PPT1 might play an important role in starch and sucrose metabolism. It is probably an important gene controlling the starch properties in sweet potato. These findings will help to elucidate the genetic basis and regulatory mechanisms underlying starch properties in sweet potato.

Materials And Methods

Plant material and growth conditions

The sweet potato varieties Xushu22 (XS22) was cultivated at temperatures of between 22 and 28°C in the experimental base of the Sweet Potato and Potato Research Institute, Southwest University, Chongqing, China. Leaf, stem, petiole, and root were sampled at 95 days after transplanting (DAP) and quickly frozen in liquid nitrogen then stored at -80°C until use for RNA extraction. All *Arabidopsis thaliana* and *Nicotiana benthamiana* plants were grown in a 22°C and 28°C climate chamber (16h light/8 dark) in Longping experimental building, Southwest University, Chongqing, China.

Cloning sweet potato GPT genes and sequence analysis

To obtain the full-length mRNA sequences of target sweet potato GPT-encoding genes, the cDNAs of *GPT* genes were cloned using the SMARTer^{TM} RACE cDNA amplification kit (Invitrogen, USA). RNA was extracted from the leaf, stem, petiole, and storage root of sweet potato variety Xushu 22 (XS22), and residual DNA was digested using the RNAprep Pure Plant Kit with DNase I (DP432, Tiangen Biotech, Beijing, China) according to the manufacturer's instructions. A 5-mg, equally proportioned (w/w) mixture of the above RNAs was used for first-strand cDNA synthesis. The gene-specific primers 83665-5-1 (5'-GGTGTGTGCAACTGCAACTGGGAAGAGGG-3') and 83665-5-2 (5'- GCCTCACAGCCGAGATCATCATTAT-3') were designed based on *IbG6PPT* transcripts (Yang et al., 2017; Zhang et al., 2017) and used to amplify the 5' end of the *GPT* genes. The primers 83665-3-1 (5'-GGTGGTTGCTCGCTTGCTGCTCTTACCG-3') and 83665-3-2 (5'-TCAGTATTGGAAACACCATGAAGCGT-3') were used to amplify the 5' and 3' ends of *GPT* genes. PCR products were cloned into the pMD19-T vector (TaKaRa) and sequenced. Based on the

obtained 5'- and 3'-end sequences of *GPT* genes, the full-length cDNA sequence was amplified using a 5' primer (5'-ACACAACACACTGTACTTGTTTC-3') and 3' primer (5'-CAAAATTTGAAAGAGTTCCCTAACAG-3') that were designed to match the 5'- and 3'-end sequences. PCR products were recombined into the Gateway entry vector pENTR-D-TOPO (Thermo Fisher, Massachusetts, USA) for sequencing. Open reading frame (ORF) and sequence alignment was performed with Geneious Prime.

Transmembrane transport peptides were predicted by the TMPred tool in ExPASy (http://www.ch.embnet.org/software/TMPRED_form.html/, (Krogh et al., 2001) and TMHMM (http://www.cbs.dtu.dk/services/TMHMM/) (Hofmann and Stoffel, 1993) using default parameters. Signal peptides were predicted by the SignalP 4.1 (http://www.cbs.dtu.dk/services/SignalP/) server using default parameters (Petersen et al., 2011). Conserved domains in the encoded proteins were analyzed with InterPro (http://www.ebi.ac.uk/interpro/) (Southan, 2000). The three-dimensional structure of IbG6PPT1 was predicted using Swiss-Model (http://www.swissmodel.expasy.org), and the constructed model was examined and visualized with Chimera 1.2 (https://www.cgl.ucsf.edu/chimera/). Multiple sequence alignment results from ClustalW were used for phylogenetic tree construction by the neighbor-joining method with MEGAX (Kumar et al., 2018). Tree reliability was measured by bootstrap analysis with 1000 replicates.

Expression pattern assay

RNA (1 μg) was extracted from the leaf, stem, petiole, and root of 95 DAP in XS22 and was reverse transcribed in a 20 μL volume by the PrimeScript RT Master Mix (TaKaRa) according to the manufacturer's instructions. The expression pattern of *GPT* genes was detected using primers and RT-qPCR methods as previously described (Zhang et al., 2017). Fold changes of the *GPT* transcripts were calculated according to the $2^{-\triangle\triangle Ct}$ method with three samples.

Subcellular localization

The full coding sequence (CDS) of *IbG6PPT1* was cloned into pCAMBIA1300, and a GFP tag was fused to the C terminus of the gene. This construct was transformed into *Agrobacterium tumefaciens* strain GV3101 and transiently expressed in *Nicotiana benthamiana* using syringe agroinfiltration (Huy et al., 2016). GFP fluorescence was observed using a Zeiss LSM780 confocal laser scanning microscope (Li et al., 2019). Signals were detected using excitation/emission wavelengths for GFP (488 nm/495–535 nm) and the chloroplast marker (633 nm/660–720 nm).

Heterologous expression of IbG6PPT1 in Arabidopsis

The full CDS of *IbG6PPT1* was recombined from the Gateway entry vector pENTR-D-TOPO (see the cloning and sequence analysis method above) into the destination vector pEarleyGate101 (Earley et al., 2006), yielding the construct *p35S*::*IbG6PPT1-YFP*, which has an N-terminal YFP tag. The construct *p35S*::*IbG6PPT1-YFP* was transformed into Arabidopsis using the *Agrobacterium tumefaciens*–mediated floral dip method (Desfeux et al., 2000).

Positive transgenic lines were identified by PCR detection of *YFP* using the primers YFP-Fwd (5'-TGGTCGAGCTGGACGGCGACGTAAAC-3') and YFP-Rev (5'-TTCTCGTTGGGGTCTTTGCTCAGGGC-3') and by detection of the *bar* gene in the construct using the primers FBar (5'-TGGGCAGCCCGATGACAGCGACCAC-3') and RBar (5'-ACCGAGCCGCAGGAACCGCAGGAGT-3'). *IbG6PPT1* expression in the transgenic Arabidopsis plants was detected using the RT-qPCR method described in the expression pattern assay section. YFP expression was detected by western blotting using an anti-GFP antibody (Welsch et al., 2019). Thousand seed weight (g) was determined for 1000 seeds from each sample with three replicates.

Starch and sugar measurement

The starch and soluble sugar contents of leaves and seeds in transgenic and control Arabidopsis plants were determined using a previously published method (Kunz et al., 2010). Briefly, leaves and roots of 3 weeks seedlings were stained with an iodine solution (2% KI+1% I_2) and examined under a light microscope (Nikon, Japan), and images were captured using NIS-Elements BR 4.30.00 software as previously described (Kunz et al., 2010).

Declarations

Author Contributions

Wu Z planed and performed the experiments and prepared the manuscript. Wang Z performed the experiments. Zhang K edited the manuscript and gave advices regarding the work. All authors have read and approved the manuscript.

Funding

This research was funded by National Key Research and Development Plan (2018YFD1000705, 2018YFD1000700), Fundamental Research Funds for the Central Universities (XDJK2020B032) and the Technology Innovation Fund of Chongqing (cstc2019jscx-msxmX0326).

Conflicts of Interest

The authors declare no conflict of interest. The funders had no role in the design of the study; in the collection, analyses, or interpretation of data; in the writing of the manuscript, or in the decision to publish the results.

Availability of data and materials

The datasets supporting the conclusions of this article are included within the article and its additional files. About proteins database could download from NCBI by their accession number.

References

[1]Andriotis VME, Pike MJ, Kular B, et al.Starch turnover in developing oilseed embryos. *New Phytol* **2010** 187: 791-804. doi: 10.1111/j.1469-8137.2010.03311.x.

[2]Baune M-C, Lansing H, Fischer K, et al.The Arabidopsis Plastidial Glucose-6-Phosphate Transporter GPT1 is Dually Targeted to Peroxisomes via the Endoplasmic Reticulum. *Plant Cell* **2020** 32: 1703-1726. doi: 10.1105/tpc.19.00959.

[3]Burri BJ.Evaluating Sweet Potato as an Intervention Food to Prevent Vitamin A Deficiency. *Compr. Rev. Food Sci. Food Saf.* **2011** 10: 118-130. doi: 10.1111/j.1541-4337.2010.00146.x.

[4]Chadee A,Vanlerberghe GC.Distinctive mitochondrial and chloroplast components contributing to the maintenance of carbon balance during plant growth at elevated CO_2. *Plant Signal. Behav.* **2020** 15: 1795395. doi: 10.1080/15592324.2020.1795395.

[5]Chen Q, Xu X, Xu D, et al.WRKY18 and WRKY53 Coordinate with HISTONE ACETYLTRANSFERASE1 to Regulate Rapid Responses to Sugar. *Plant Physiol.* **2019** 180: 2212-2226. doi: 10.1104/pp.19.00511.

[6]Desfeux C, Clough SJ,Bent AF.Female Reproductive Tissues Are the Primary Target of Agrobacterium-Mediated Transformation by the Arabidopsis Floral-Dip Method. *Plant Physiol.* **2000** 123: 895-904. doi: 10.1104/pp.123.3.895.

[7]Dyson BC, Allwood JW, Feil R, et al.Acclimation of metabolism to light in *Arabidopsis thaliana*: the glucose 6-phosphate/phosphate translocator GPT2 directs metabolic acclimation. *Plant Cell Environ.* **2015** 38: 1404-1417. doi: 10.1111/pce.12495.

[8]Earley KW, Haag JR, Pontes O, et al.Gateway-compatible vectors for plant functional genomics and proteomics. *Plant J.* **2006** 45: 616-629. doi: 10.1111/j.1365-313X.2005.02617.x.

[9]Fan Y, Yu M, Liu M, et al.Genome-Wide Identification, Evolutionary and Expression Analyses of the *GALACTINOL SYNTHASE* Gene Family in Rapeseed and Tobacco. *Int. J. Mol. Sci.* **2017** 18: 2768. doi: 10.3390/ijms18122768.

[10]Gao M, Soriano SF, Cao Q, et al.Hexaploid sweetpotato (*Ipomoea batatas* (L.) Lam.) may not be a true type to either auto- or allopolyploid. *PloS One* **2020** 15: e0229624. doi: 10.1371/journal.pone.0229624.

[11]Hofmann K,Stoffel W.TMbase - A database of membrane spanning proteins segments. *Biol. Chem. Hoppe-Seyler* **1993** 374: 166. doi: 10.1515/bchm3.1993.374.1-6.143

[12]Hu J, Nakatani M, Lalusin AG, et al.Genetic Analysis of Sweetpotato and Wild Relatives using Inter-simple Sequence Repeats (ISSRs). *Breed. Sci.* **2003** 53: 297-304. doi: 10.1270/jsbbs.53.297.

[13]Huy N-X, Tien N-Q-D, Kim M-Y, et al.Immunogenicity of an S1D epitope from porcine epidemic diarrhea virus and cholera toxin B subunit fusion protein transi-ently expressed in infiltrated *Nicotiana benthamiana* leaves. *Plant Cell, Tissue Organ Cult.* **2016** 127: 368-380. doi: 10.1007/s11240-016-1059-5.

[14]Jack DL, Yang NM,H. Saier M.The drug/metabolite transporter superfamily. *Eur. J Biochem.* **2001** 268: 3620-3639. doi: 10.1046/j.1432-1327.2001.02265.x.

[15]Koçar G,Civaş N.An overview of biofuels from energy crops: Current status and future prospects. *Renewable Sustainable Energy Rev.* **2013** 28: 900-916. doi: 10.1016/j.rser.2013.08.022.

[16]Krogh A, Larsson B, Heijne Gv, et al.Predicting transmembrane protein topology with a hidden markov model: application to complete genomes. *J. Mol. Biol.* **2001** 305: 567-580. doi: 10.1006/jmbi.2000.4315.

[17]Kumar S, Stecher G, Li M, et al.MEGA X: Molecular evolutionary genetics analysis across computing platforms. *Mol. Biol. Evol.* **2018** 35: 1547-1549. doi: 10.1093/molbev/msy096.

[18]Kunz HH, Häusler RE, Fettke J, et al.The role of plastidial glucose-6-phosphate/phosphate translocators in vegetative tissues of Arabidopsis thaliana mutants impaired in starch biosynthesis. *Plant Biol.* **2010** 12: 115-128. doi: 10.1111/j.1438-8677.2010.00349.x.

[19]Lai YC, Wang SY, Gao HY, et al.Physicochemical properties of starches and expression and activity of starch biosynthesis-related genes in sweet potatoes. *Food Chem.* **2016** 199: 556-564. doi: 10.1016/j.foodchem.2015.12.053.

[20]Lee E-J, Oh M, Hwang J-U, et al.Seed-Specific Overexpression of the Pyruvate Transporter *BASS2* Increases Oil Content in *Arabidopsis* Seeds. *Front. Plant Sci.* **2017** 8: 194. doi: 10.3389/fpls.2017.00194.

[21]Li J, Chen F, Li Y, et al.ZmRAP2.7, an AP2 Transcription Factor, Is Involved in Maize Brace Roots Development. *Front. Plant Sci.* **2019** 10: 820. doi: 10.3389/fpls.2019.00820.

[22]Mitra S.Nutritional Status of Orange-Fleshed Sweet Potatoes in Alleviating Vitamin A Malnutrition through a Food-Based Approach. *J. Nutr. Food Sci.* **2012** 2: 160. doi: 10.4172/2155-9600.1000160.

[23]Nedunchezhiyan M, Byju G,Jata SK.Sweet potato agronomy. *Fruit, Vegetable and Cereal Science and Biotechnology* **2012** 6: 1-10.

[24]Niewiadomski P, Knappe S, Geimer S, et al.The Arabidopsis Plastidic Glucose 6-Phosphate/Phosphate Translocator GPT1 Is Essential for Pollen Maturation and Embryo Sac Development. *Plant Cell* **2005** 17: 760-775. doi: 10.1105/tpc.104.029124.

[25]Petersen TN, Brunak S, Heijne Gv, et al.SignalP 4.0: discriminating signal peptides from transmembrane regions. *Nat. Methods* **2011** 8: 785-786. doi: 10.1038/nmeth.1701.

[26]Qu A, Xu Y, Yu X, et al.Sporophytic control of anther development and male fertility by glucose-6-phosphate/phosphate translocator 1 (*OsGPT1*) in rice. *J. Genet. Genomics* **2021** doi: 10.1016/j.jgg.2021.04.013.

[27]Rolletschek H, Nguyen TH, Häusler RE, et al.Antisense inhibition of the plastidial glucose-6-phosphate/phosphate translocator in *Vicia* seeds shifts cellular differentiation and promotes protein storage. *Plant J.* **2007** 51: 468-484. doi: 10.1111/j.1365-313X.2007.03155.x.

[28]Schreiber L, Nader-Nieto AC, Schönhals EM, et al.SNPs in genes functional in starch-sugar interconversion associate with natural variation of tuber starch and sugar content of potato (*Solanum tuberosum L.*). *G3 (Bethesda)* **2014** 4: 1797-1811. doi: 10.1534/g3.114.012377.

[29]Southan C.InterPro (The Integrated Resource of Protein Domains and Functional Sites). *Yeast* **2000** 17: 327-334. doi: 10.1002/1097-0061(200012)17:4<327::AID-YEA45>3.0.CO;2-K.

[30]Srichuwong S, Orikasa T, Matsuki J, et al.Sweet potato having a low temperature-gelatinizing starch as a promising feedstock for bioethanol production. *Biomass Bioenergy* **2012** 39: 120-127. doi: 10.1016/j.biombioe.2011.12.023.

[31]Wang H, Wu Y, Zhang Y, et al.CRISPR/Cas9-Based Mutagenesis of Starch Biosynthetic Genes in Sweet Potato (Ipomoea Batatas) for the Improvement of Starch Quality. *Int. J. Mol. Sci.* **2019** 20: 4702. doi: 10.3390/ijms20194702.

[32]Weise SE, Liu T, Childs KL, et al.Transcriptional Regulation of the Glucose-6-Phosphate/Phosphate Translocator 2 Is Related to Carbon Exchange Across the Chloroplast Envelope. *Front. Plant Sci.* **2019** 10: 827. doi: 10.3389/fpls.2019.00827.

[33]Welsch R, Zhou X, Koschmieder J, et al.Characterization of Cauliflower OR Mutant Variants. *Front. Plant Sci.* **2019** 10: 1716. doi: 10.3389/fpls.2019.01716.

[34]Wesemael Jv, Hueber Y, Kissel E, et al.Homeolog expression analysis in an allotriploid non-model crop via integration of transcriptomics and proteomics. *Sci. Rep.* **2018** 8: 1353. doi: 10.1038/s41598-018-19684-5.

[35]Winter H,Huber SC.Regulation of Sucrose Metabolism in Higher Plants: Localization and regulation of Activity of Key Enzymes. *CRC Cri. Rev. Plant Sci.* **2000** 19: 31-67. doi: 10.1080/07352680091139178.

[36]Yang D, Xie Y, Sun H, et al.IbINH positively regulates drought stress tolerance in sweetpotato. *Plant Physiol. Biochem.* **2020** 146: 403-410. doi: 10.1016/j.plaphy.2019.11.039.

[37]Yang J, Moeinzadeh M-H, Kuhl H, et al.Haplotype-resolved sweet potato genome traces back its hexaploidization history. *Nat. Plants* **2017** 3: 696-703. doi: 10.1038/s41477-017-0002-z.

[38]Zhang H, Zhang Q, Zhai H, et al.IbBBX24 Promotes the Jasmonic Acid Pathway and Enhances Fusarium Wilt Resistance in Sweet Potato. *Plant Cell* **2020** 32: 1102-1123. doi: 10.1105/tpc.19.00641.

[39]Zhang K, Wu Z, Tang D, et al.Comparative Transcriptome Analysis Reveals Critical Function of Sucrose Metabolism Related-Enzymes in Starch Accumulation in the Storage Root of Sweet Potato.

Front. Plant Sci. **2017** 8: 914. doi: 10.3389/fpls.2017.00914.

[40]Zheng Y, Deng X, Qu A, et al.Regulation of pollen lipid body biogenesis by MAP kinases and downstream WRKY transcription factors in Arabidopsis. *PLoS Genet.* **2018** 14: e1007880. doi: 10.1371/journal.pgen.1007880.

[41]Zhou W, Yang J, Hong Y, et al.Impact of amylose content on starch physicochemical properties in transgenic sweet potato. *Carbohydr, Polym.* **2015** 122: 417-427. doi: 10.1016/j.carbpol.2014.11.003.

Figures

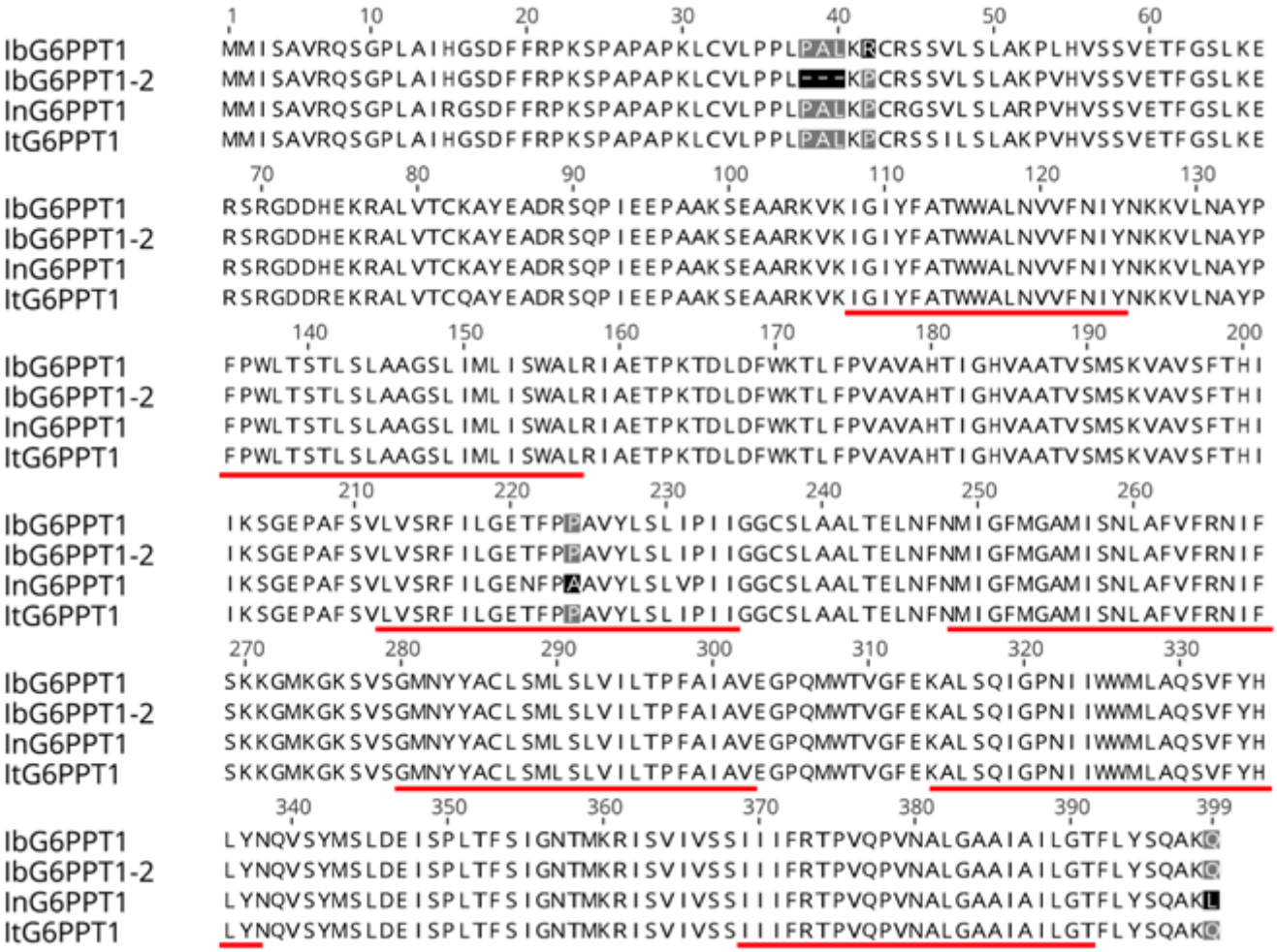

Figure 1

Alignment of IbG6PPT1, IbG6PPT1-2, and Ipomoea genus GPT1 proteins. ItG6PPT1, Ipomoea triloba GPT1 (XP_031105621.1); InG6PPT1, Ipomoea nil G6PPT1 (XP_019193616.1). The amino acids underlined in red form transmembrane helixes based on prediction using TMHMM; black and grey highlighting indicate amino acid differences between the species.

Figure 2

Phylogenetic analysis of GPT proteins. The phylogenetic tree was constructed using the Neighbor-Joining method implemented in MEGA-X software. The numbers on the branches are bootstrap values (based on 1,000 repeats).

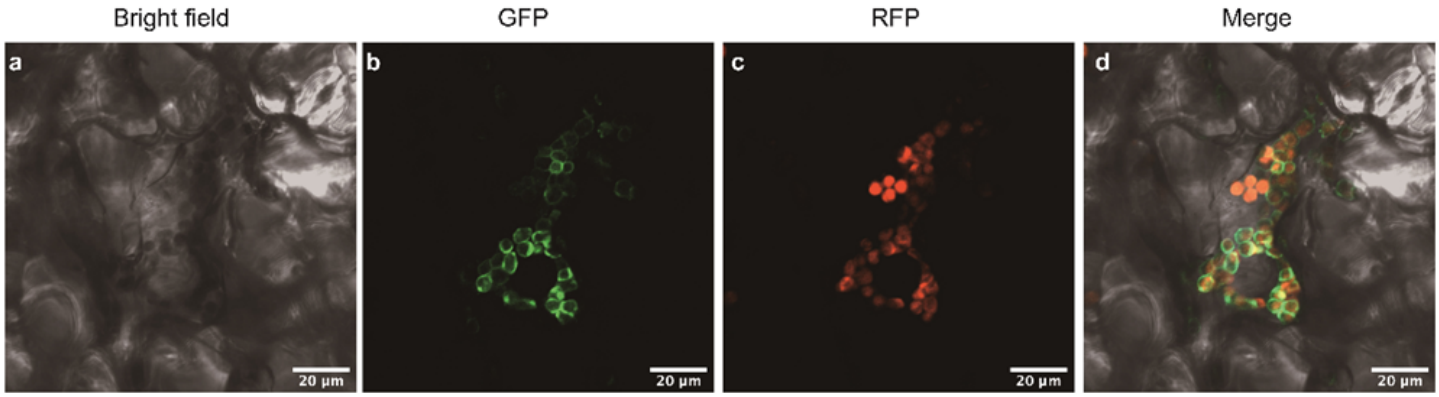

Figure 3

IbG6PPT1 localizes to the chloroplast membrane. (a) Nicotiana benthamiana leaf viewed in bright field, (b) IbG6PPT1-YFP viewed in the green channel, (c) the chloroplast marker viewed in the red channel, and (d) the merged images illustrating the localization of IbG6PPT1 to the chloroplast membrane.

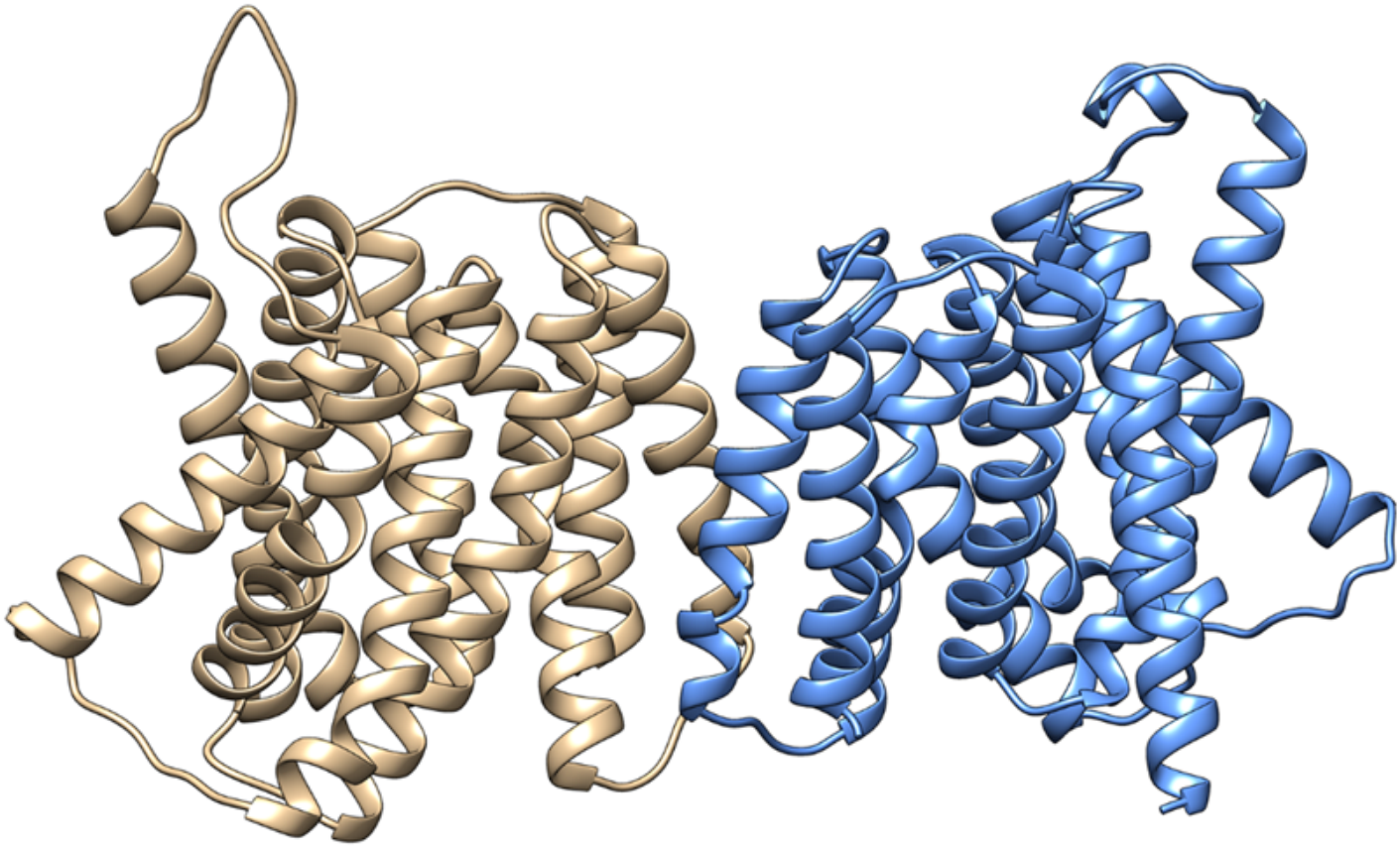

Figure 4

Predicted three-dimensional structure models of IbG6PPT1. Two IbG6PPT1 proteins (shown in yellow and blue) form a dimer.

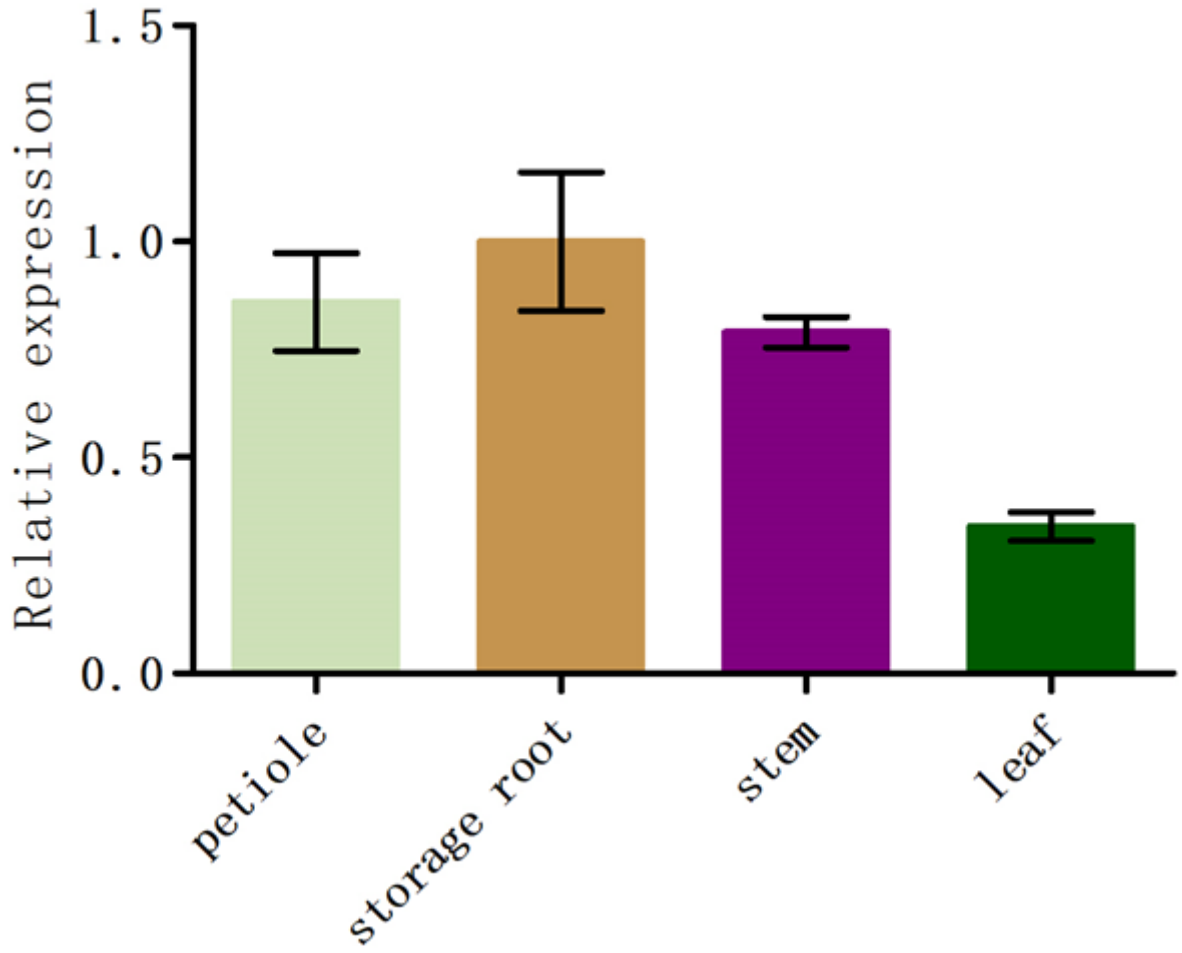

Figure 5

Expression of IbG6PPT1 in the petiole, storage root, stem, and leaf of the sweet potato variety Xushu 22, as determined by qRT-PCR. Each value is the mean±SD of at least three independent measurements.

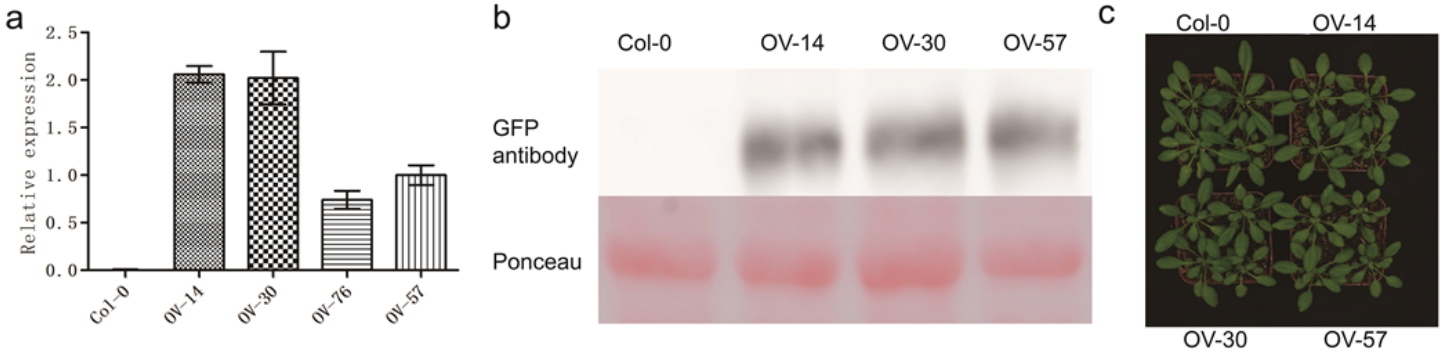

Figure 6

Heterologous expression of IbG6PPT1 in Arabidopsis. (a) qRT-PCR detection of IbG6PPT1 expression; each value is the mean±SD of at least three independent measurements. (b) Western blot detection of

IbG6PPT1 expression. (c) Phenotype of 4 weeks Arabidopsis plants heterologously expressing IbG6PPT1. Col-0, control plants; OV-14, OV-30, OV-76, and OV-57, four transgenic lines.

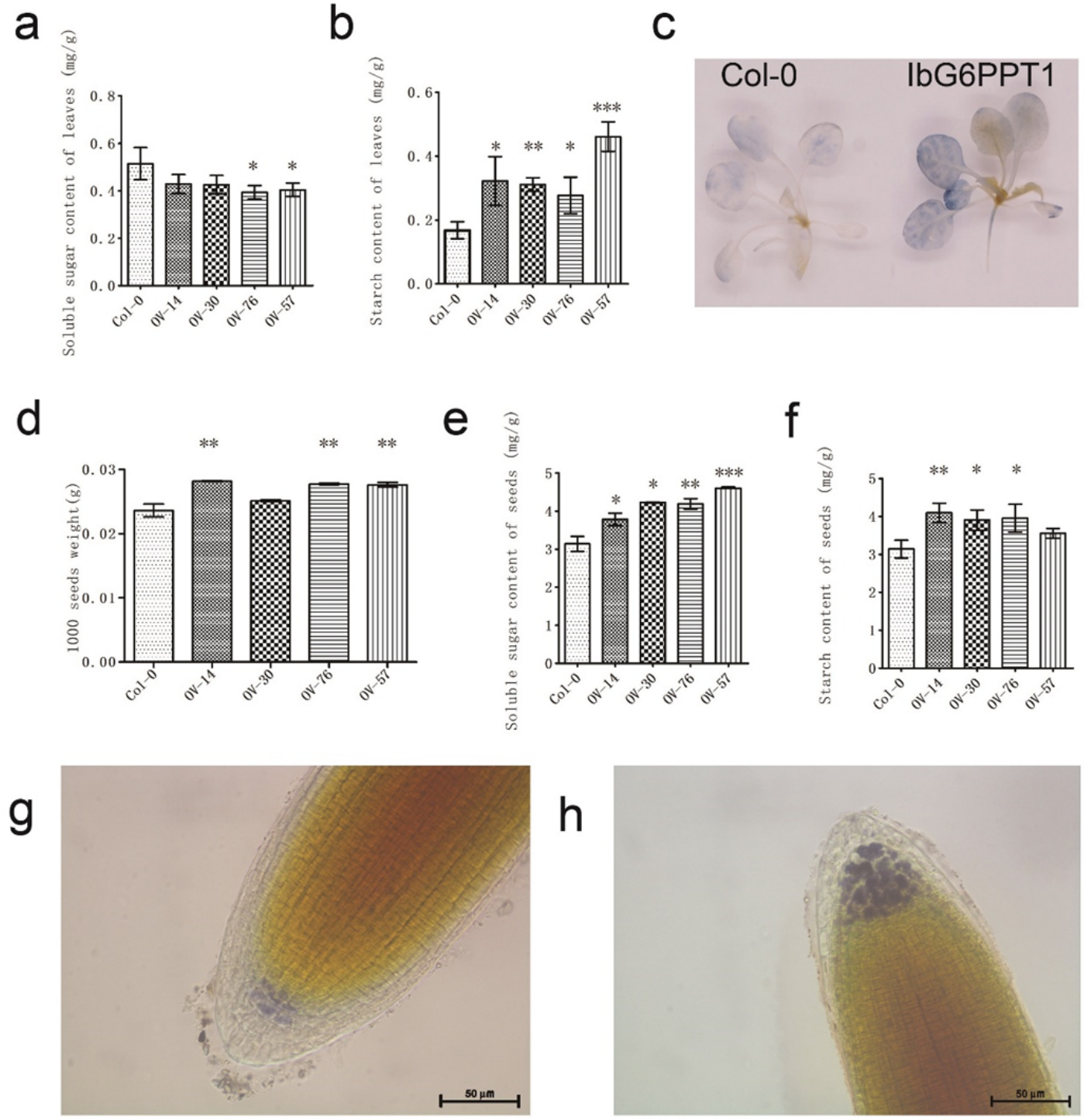

Figure 7

Heterologous expression of IbG6PPT1 in Arabidopsis alters the starch and soluble sugar content of the plants. (a) Soluble sugar content and (b) Starch content of the leaves of 6 weeks Arabidopsis plants. (c) Iodine-stained starch in the leaves of 3 weeks seedings. (d) weight in 1000 seed, (e) soluble sugar content and (f) starch content in the seed in the transgenic and control plants. (g) and (h), Iodine-stained starch in

the root tips of control and transgenic plants, respectively. Col-0, control plants; OV-14, OV-30, OV-76, and OV-57, four transgenic lines. Each value is the mean±SD of at least three independent measurements.

Supplementary Files

This is a list of supplementary files associated with this preprint. Click to download.

- TableS1.xlsx